

Fermi surface and interlayer transport in high-stage MoCl_5 graphite intercalation compounds

Kengo Enomoto,* Shinya Uji, Takahide Yamaguchi, Taichi Terashima, Takako Konoike, and Mitsuka Nishimura
National Institute for Materials Science, Tsukuba, Ibaraki 305-0003, Japan

Toshiaki Enoki
Tokyo Institute of Technology, Meguro-ku, Tokyo 152-8551, Japan

Masatsugu Suzuki and Itsuko S. Suzuki
State University of New York at Binghamton, Binghamton, New York 13902-6000, USA
(Received 12 July 2005; revised manuscript received 13 October 2005; published 18 January 2006)

Shubnikov–de Haas (SdH) and angular-dependent magnetoresistance oscillations (AMRO's) in high-stage MoCl_5 graphite intercalation compounds are reported. Several SdH oscillations and AMRO's are observed; however, the background of the angular-dependent magnetoresistance cannot be interpreted by the semiclassical model based on the Boltzmann coherent transport theory. A resistance peak in magnetic fields parallel to the conducting layers is clearly observed, demonstrating coherent transport. The results are discussed in terms of an incoherent motion crossing the magnetic intercalate layers and a coherent motion only in the graphite layers.

DOI: [10.1103/PhysRevB.73.045115](https://doi.org/10.1103/PhysRevB.73.045115)

PACS number(s): 71.20.Tx, 72.15.Gd

I. INTRODUCTION

The interlayer magnetoresistance, which shows angular effects as a function of magnetic field orientation, has been extensively studied in layered quasi-one-dimensional¹ (Q1D) and quasi-two-dimensional^{2,3} (Q2D) conductors. In these conductors, one of the most fundamental concepts of the electronic transport is based on the coherent motion of electrons in energy bands or Bloch states. In this model, it is tacitly assumed that the coherent interlayer transport allows an electron to tunnel through many layers without scattering. The theoretical model predicts the observation of a resistance peak in magnetic fields (B) parallel to the layers and the relation $R(B\parallel\text{layers}) > R(B\perp\text{layers})$ in the angular-dependent magnetoresistance. However, in some cases, such a simple semiclassical Boltzmann transport theory fails and a more generalized transport theory has been proposed.⁴ For Q2D systems, the theoretical studies argue that the standard angular-dependent magnetoresistance oscillation (AMRO) could appear even in a system where the interlayer transport is weakly incoherent. Incoherent interlayer transport is expected in the inequality $\hbar/\tau > t_c$, where τ^{-1} and t_c is the intralayer scattering rate and the interlayer hopping integral, respectively. In this situation, a resistance peak in magnetic fields parallel to the layers is not observable since the Fermi surface is only defined within the layers and the interlayer conductivity is proportional to the tunneling rate between two adjacent layers.⁴ The theoretical studies also reveal that the background of the angular-dependent magnetoresistance is identical to that in the coherent case, i.e., $R(B\parallel\text{layers}) > R(B\perp\text{layers})$. Indeed, the incoherent nature of interlayer transport is supported by the absence of a peak in fields parallel to the layers in a highly two-dimensional (2D) superconductor $\beta''\text{-(BEDT-TTF)}_2\text{SF}_5\text{CH}_2\text{CF}_2\text{SO}_3$ [where BEDT-TTF is the organic molecule bis(ethylenedithio)-tetrathiafulvalene].⁵ On the other hand, a discrepancy of the

criterion is found in some Q2D BEDT-TTF salts. The well-known superconductor $\kappa\text{-(BEDT-TTF)}_2\text{Cu(NCS)}_2$ meets the criterion of incoherent interlayer transport ($\hbar/\tau \sim 6t_c$) while it clearly shows a sharp peak when magnetic fields are parallel to the conducting layers.^{6,7} A similar observation was reported for the isostructural superconductor $\kappa\text{-(BEDT-TTF)}_2\text{I}_3$.⁵ Thus, the applicability of the criterion of incoherent transport to highly anisotropic systems was questioned.^{6,8} On the other hand, the anomalous background [$R(B\parallel\text{layers}) < R(B\perp\text{layers})$] has been observed for Q1D (TMTSF)₂X (where TMTSF is tetramethyltetraselenafulvalene⁹⁻¹¹) and artificial Q2D GaAs/AlGaAs superlattices with different interlayer barriers.¹² This anomalous background is interpreted in terms of an incoherent interlayer transport. Other comparative experimental studies of the coherent versus incoherent interlayer transport have been carried out on Q2D (BEDT-TTF)₂Br(DIA) (where DIA is diiodoacetylene).¹³ As far as we know, however, the comprehensive understanding of the coherent-incoherent issues has not been achieved yet.

To further investigate the above issues, acceptor-type graphite intercalation compounds (GIC's) were selected, since these compounds might be one of the potential candidates for displaying interesting effects in these issues. GIC's also have Q2D layered structures and the interlayer periodic structures are characterized by the stage number n .^{14,15} Stage n means that the intercalates are accommodated regularly between n graphite layers. The interlayer repeat distance I_c is given by

$$I_c = d_I + (n - 1)d_G, \quad (1)$$

where d_I and d_G are the thicknesses of the intercalate layer and the interlayer distance ($=3.35 \text{ \AA}$) for the pristine graphite, respectively. The staging structure is well controlled by the synthetic condition. For acceptor-type GIC's, the inter-

layer conductivity becomes highly anisotropic because the intercalation always leads to a considerable increase in the spacing between graphite layers.^{14,15} Due to this highly anisotropic conductivity, some models of interlayer transport for these systems have been proposed. One is a model based on Q2D electronic states where the interlayer transport is governed by hopping conduction,^{16–18} the other is a 3D band model with large anisotropy.¹⁹ The interlayer transport in FeCl₃ GIC's has been analyzed in terms of variable-range hopping conduction in parallel with band conduction.²⁰ Thus, in acceptor-type GIC's, the mechanism of interlayer transport is still controversial.

Among various acceptor-type GIC's, MoCl₅ GIC's are the one of the most popular compounds whose magnetic and transport properties have been well studied theoretically and experimentally over the last two decades.^{18,21–24} We have performed magnetoresistance measurements in high-stage MoCl₅ GIC's, and found that the angular-dependent magnetoresistance has an anomalous background while a peak in magnetic fields parallel to the conducting layers is observed in higher-stage compounds. In this paper, we mainly report the magnetotransport properties of stage-5 MoCl₅ GIC's and discuss the interlayer transport in this compound.

II. EXPERIMENT

Samples for the present measurements were synthesized from highly oriented pyrolytic graphite (Union Carbide). The details of the synthetic condition are described in the literatures.^{21–23} The sample has a rectangular form with typically a base 0.7×0.7 mm² and a height 0.2 mm along the *c* axis. Four gold wires ($\phi=20$ μm) were attached to each of the *ab* surfaces of the samples by silver paste. The resistance was measured by a conventional four-probe ac technique with electric current (typically 20 μA) along the *c* axis, which is perpendicular to the conducting (*ab*) plane. The samples were cooled down by a ⁴He or ³He cryostat with superconducting magnets at NIMS.

III. RESULTS

Figure 1(a) shows the field dependence of interlayer resistance of a stage-5 MoCl₅ GIC at two field directions $\theta = 0^\circ$ and 90° , where θ is the angle between the field and the *c* axis. The interlayer resistance shows a relation $R_c(\theta=0^\circ) > R_c(\theta=90^\circ)$ over the whole field region. At $\theta=0^\circ$, Shubnikov–de Haas (SdH) oscillations are clearly seen above $B \sim 2$ T. The Fourier transform (FT) spectrum of the SdH oscillations is presented in Fig. 1(b). The spectrum shows three strong peaks at $\alpha=21.6$, $\beta=145$, and $\gamma=588$ T, which correspond to Fermi cylinder radii of $k_\alpha=0.026$, $k_\beta=0.066$, and $k_\gamma=0.134$ Å⁻¹, respectively, if circular cross sections are assumed. There are also still other peaks; however, they can be interpreted as harmonics and combined frequencies. The cross-sectional area of the original first Brillouin zone (BZ) in the graphite layers is estimated to be 7.53 Å⁻². If the original BZ is reconstructed by the superlattice of the intercalates, the zone folding produces overlaps between the Fermi surfaces (FS's) placed in the original BZ.

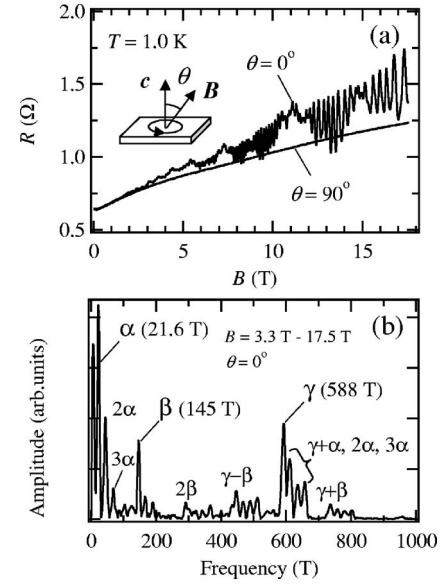


FIG. 1. (a) Field dependence of the interlayer resistance of stage-5 MoCl₅ GIC at 1.0 K. Shubnikov–de Haas oscillations are observed at $\theta=0^\circ$. Angle θ is defined in the inset. (b) Fourier transform spectrum of the SdH oscillations.

This reconstruction fractionalizes the original FS into small pockets. Such reconstruction has been reported in some GIC's; stage-2 SbCl₅ GIC (Ref. 25) and stage-2 InCl₃ GIC.²⁶ In this compound, the frequencies can also be ascribed to this effect, i.e., the small closed pockets formed by the reconstruction of the original π bands of the graphite layers due to the formation of a superlattice of the intercalates. However, it is reported that adjacent MoCl₅ intercalate layers are structurally uncorrelated in high-stage MoCl₅ GIC's.²² This makes it difficult to undertake further analysis.

Figure 2 shows the FT amplitudes of the SdH oscillations divided by temperature vs temperature plots for three frequencies. The solid lines are the fitted results with Lifshitz-Kosevich formula.²⁷ The determined effective masses m_{eff} for α , β , and γ are $0.05m_0$, $0.04m_0$, and $0.12m_0$, respectively, where m_0 is the free-electron mass. These small effective masses agree with the results in other GIC's,^{14,28} and are a consequence of the linear energy dispersion feature around

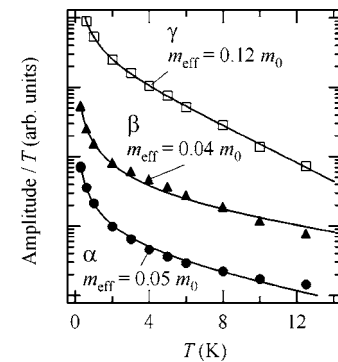


FIG. 2. FT amplitudes of the SdH oscillations divided by temperature vs temperature. The solid lines are the fitted results with the Lifshitz-Kosevich formula.

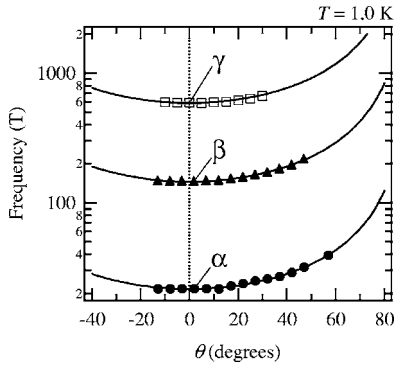


FIG. 3. SdH frequencies as a function of the magnetic field angle θ . The solid lines show $1/\cos \theta$ dependences.

the Fermi energy as described in the literature.¹⁵ Since the most of the electrons remains on the large FS (γ), the transport properties should be dominated by the electrons on the γ orbit. The Dingle temperature of the SdH oscillation is estimated to be ~ 9.7 K for γ . This value gives $\omega_c \tau = 1.9$ at 10 T, where ω_c and τ is the cyclotron frequency and scattering time, respectively. The value of $\omega_c \tau \geq 1$ is consistent with the observation of the SdH oscillation in this compound.

Figure 3 shows the SdH frequencies as a function of the field angle θ . The solid lines are calculated $1/\cos \theta$ dependences expected for the cylindrical FS's. The good agreement with the experimental results shows that all the frequencies arise from the cylindrical FS's. Even for γ , the beat behavior due to the maximum and minimum cross-sectional areas of the Q2D FS is not resolved in the wide range of magnetic fields between 3.3 and 17.5 T [Fig. 1(b)]. The result indicates that the cylindrical FS is hardly corrugated along the c axis.

Figure 4(a) shows the angular-dependent magnetoresistance for different fields at $T=1.7$ K. A remarkable point is that the relation $R(\theta=0^\circ) > R(\theta=90^\circ)$ is observed while the semiclassical magnetotransport theory predicts the maximum value at $\theta=90^\circ$ due to the maximum Lorentz force in this direction. The anomalous background is observed over the whole field region. We discuss this point later. Figure 4(b) shows the resistance normalized by the peak value $R(\theta=90^\circ)$. In addition to the anomalous background, sharp peaks are visible at $\theta=90^\circ$. Since no SdH oscillations are observed at $T=1.7$ K for $\theta \sim 90^\circ$ [cf. Fig. 1(a)], these peaks do not arise from the SdH oscillations. The peak shape and its angular width are independent of the field strength above $B \sim 3$ T. Similar peak structures have been reported for β -(BEDT-TTF)₂I₃ and α -(BEDT-TTF)₂NH₄Hg(SCN)₄.²⁹ The width of the peak $\Delta\theta_{\text{peak}}$ is defined as the angle region between the two inflection points [see also Fig. 6(b)].

As mentioned, the standard AMRO could appear in both coherent interlayer transport and weakly incoherent interlayer transport.⁴ In Fig. 4(a), the oscillatory behavior in the low-angle region is caused by the SdH oscillations which remain until $T \sim 30$ K. At higher angles, however, a series of the distinct peaks are identified [Fig. 4(b)]. The resistance peaks indicated by arrows do not shift as the field increases but merely grow in amplitude. The result shows that the oscillatory behavior is not caused by the quantum oscillation,

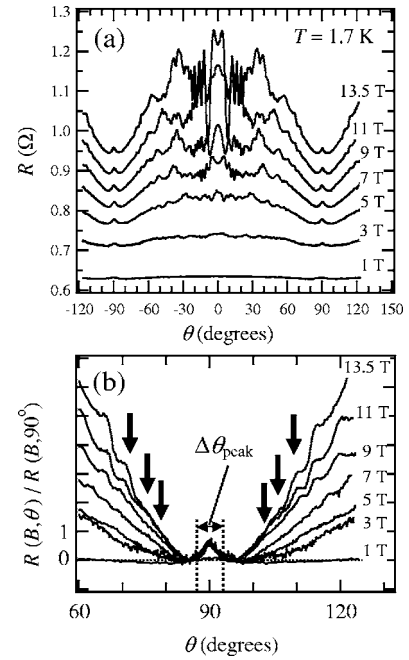


FIG. 4. (a) Angular-dependent magnetoresistance for different magnetic fields at $T=1.7$ K. (b) The normalized curves $R(B, \theta)/R(B, 90^\circ)$ for magnetic fields close to the conducting layers. The arrows denote the AMRO peaks.

but by the AMRO which was firstly discovered in a Q2D organic conductor.³⁰ Figure 5 shows the second-derivative curve of the AMRO as a function of $\tan \theta$ measured at $T=1.7$ K and $B=13.5$ T. A periodic structure due to the AMRO is clearly observed in the high-angle region while the oscillatory behavior for $|\tan \theta| \leq 2.5$ corresponds to SdH oscillations [Fig. 4(a)]. The standard model predicts that the peaks appear at the angles defined by³¹

$$I_c k_F \tan \theta = \pi(n - 1/4), \quad (2)$$

where k_F and n are the Fermi wave number and arbitrary integer numbers, respectively. Although this formula has been first derived for the Q2D coherent systems, it is even valid for Q2D weakly incoherent systems.⁴ When we put $I_c = 22.83 \text{ \AA}$ for a stage-5 MoCl₅ GIC,²³ we can evaluate the radius of the Fermi cylinder as $k_F \sim 0.13 \text{ \AA}^{-1}$. The Fermi

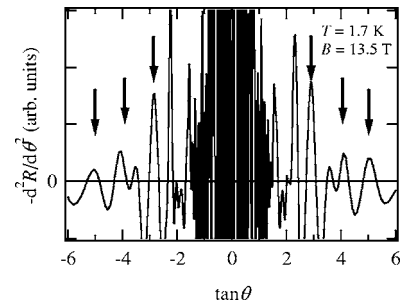


FIG. 5. Second-derivative curve of AMRO as a function of $\tan \theta$. The oscillatory behavior at $|\tan \theta| \leq 2.5$ is caused by the SdH oscillations. The arrows correspond to the AMRO peaks presented in Fig. 4(b).

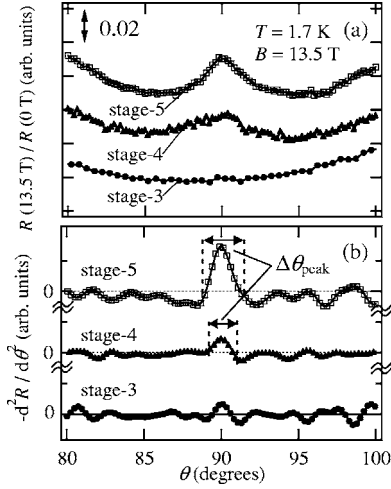


FIG. 6. (a) Interlayer resistance close to $\theta=90^\circ$ for stages-3, -4, and -5 MoCl_5 GIC's. (b) Second-derivative curves of the resistance. Each curve is shifted for clarity.

cylinder radius of 0.13 \AA^{-1} coincides with k_γ determined by the SdH measurements. Therefore, the FS obtained from the AMRO measurements is assigned to that corresponding to the frequency γ . The angular-dependent magnetoresistances for various in-plane azimuthal angles ϕ (ϕ dependence) were also examined. But no variation of the AMRO features with various azimuthal angles was seen, suggesting that the cross section of the FS is almost circular.

Figure 6(a) shows the interlayer resistance close to $\theta=90^\circ$ for stages-3, -4, and -5 MoCl_5 GIC's. The anomalous background is also observed for stages-3 and -4 MoCl_5 GIC's. The second-derivative curves $-d^2R/d\theta^2$ of the resistance are shown in Fig. 6(b). We note that the peak at $\theta=90^\circ$ is less evident for the stage-3 MoCl_5 GIC. The stage-2 MoCl_5 GIC shows a similar anomalous background; however, it no longer shows the peak at $T=1.7 \text{ K}$ and $B=13.5 \text{ T}$ (not shown). The results suggest that the peak at $\theta=90^\circ$ is highly correlated with the thickness of the graphite layers.

IV. DISCUSSION

We first discuss the anomalous feature of the magnetoresistance found in these compounds. Even in the case of weakly incoherent transport, it is theoretically argued that the background of the angular-dependent magnetoresistance is identical to that in the coherent case, i.e., it increases monotonically from $\theta=0^\circ$ to 90° and saturates at $\theta\sim 90^\circ$. The only difference in the angular dependence between the coherent and weakly incoherent transport cases is whether the peak at $\theta=90^\circ$ is observed or not.⁴ Therefore, the anomalous background as shown in Fig. 4 is not understood by their models. Similar anomalous background has been reported for $(\text{TMTSF})_2\text{PF}_6$ at high pressures,⁹⁻¹¹ GaAs/AlGaAs semiconductor superlattices,¹² and some other magnetic GIC's.^{32,33}

For Q1D electronic systems $(\text{TMTSF})_2X$ ($X=\text{ClO}_4, \text{PF}_6$, etc.), the magnetoresistance and its angular dependence

have been extensively studied theoretically and experimentally.^{1,9-11} These salts belong to a family of highly anisotropic organic conductors with the bandwidth along the crystal axes given by $4t_a:4t_b:4t_c\sim 1:0.1:0.003 \text{ eV}$. When the magnetic field is aligned along the intermediate conducting b direction, the interlayer magnetoresistance (R_{zz}) in the PF_6 salt has the minimum value whereas the semiclassical model predicts that R_{zz} has the maximum value because of the maximum Lorentz force in this direction. At high fields along the b direction, the electron is effectively confined to a single layer and then the layers are decoupled along the c axis. This is the dimensional crossover or interlayer decoupling. This dimensional crossover on decoupling caused by the in-plane field makes the interlayer transport incoherent while it keeps the in-plane transport coherent. The minimum in R_{zz} has been interpreted in terms of this incoherent transport and a universal power law for $R_{zz}(B)-R_{zz}(0)\propto B^{3/2}$ is observed.^{10,11}

For GaAs/AlGaAs semiconductor superlattices, the interlayer coupling is well controlled by the barrier width.¹² The usual AMRO and the peak at $\theta=90^\circ$ are clearly observed on the narrow-barrier sample, i.e., the system holds interlayer coherence. On the other hand, when the system loses interlayer coherence (with the larger barrier), the usual AMRO is observed while it shows an anomalous background with no peaks close to $\theta=90^\circ$.¹² The anomalous background becomes evident in the field region where the diameter of the classic cyclotron orbit at $\theta=90^\circ$ becomes smaller than the well width.

In the case of Q2D systems, the interlayer decoupling can also take place in a sufficiently high field parallel to the conducting layers. In the in-plane field, the electron sweeps across the Brillouin zones in the k_z direction with a frequency Ω_c given by¹¹

$$\Omega_c = (dk_z/dt)I_c \approx \frac{eB}{m_\perp} I_c k_F, \quad (3)$$

where I_c is the interlayer repeat distance, m_\perp is the mass for the k_z direction, and k_F is the in-plane component of the Fermi wave number perpendicular to the magnetic field. In real space, the electron moves sinusoidally in the interlayer direction making excursions of amplitude $(4t_c/\hbar\Omega_c)I_c$, where t_c is the interlayer transfer integral.¹¹ The interlayer decoupling can happen when $\hbar\Omega_c \geq t_c$, since the amplitude becomes smaller than I_c . As theoretically predicted, however, the decoupling may take place even for $\hbar\Omega_c < t_c$ due to electron correlation effects in the layers.⁹ For $(\text{BEDT-TTF})_2\text{Br}(\text{DIA})$, the magnetoresistance features at $\theta=90^\circ$ have been interpreted in terms of this decoupling effect and incoherent transport.¹³ Even for Q2D systems MoCl_5 GIC's, a similar interlayer decoupling may happen at high fields parallel to the conducting layers and the anomalous background in the magnetoresistance may appear above the decoupling field.

A similar anomalous background has been observed in some other magnetic GIC's,^{32,33} whereas a classical background is robust in nonmagnetic SbCl_5 GIC's (stages 2 and 3).³⁴ The origin of the anomalous background might be ex-

plained by an incoherent scattering at stacking faults and defects in these compounds. Moreover, it should be noted that the adjacent MoCl_5 layers are structurally uncorrelated in such high-stage MoCl_5 GIC's.²² This means that the intercalate layers form a random potential for the interlayer transport. At present, we cannot estimate how large the random potential is. If the randomness is fairly large, it may make the interlayer transport incoherent. We cannot rule out the possibility that the nonmagnetic scattering by the intercalate random potential is also the origin of the incoherent transport. However, this may not be the only reason since the anomalous background seems characteristic of magnetic GIC's. In magnetic $M\text{Cl}_2$ GIC's ($M=\text{Cu}$ and Co ; stages 1 and 2), the anomalous features of the magnetoresistance have been discussed in terms of spin-dependent transfer interaction which makes a larger contribution to interlayer transport than in-plane transport, and interpreted as incoherent interlayer transport.³² The above explanation may also be appropriate for other magnetic GIC's. In stages 2 to 5 MoCl_5 GIC's ($S=1/2$), the magnetic properties have been studied by ac and dc magnetic susceptibilities^{21,23} and the successive magnetic phase transitions have been observed below $T_c \sim 1.6$ K. These transitions indicate a 3D magnetic order with finite exchange interaction between the conduction π electrons and the localized Mo^{5+} ($S=1/2$) spins in these compounds. The positive Curie-Weiss temperature Θ much larger than T_c ($\Theta \lesssim \sim 15$ K) has been explained in terms of a spin fluctuation effect in the MoCl_5 intercalate layers.²³ In contrast to the nonmagnetic SbCl_5 GIC's, the existence of the magnetic fluctuation of the Mo^{5+} spins can destroy the interlayer coherence because of the magnetic scattering between the conduction π electrons and the localized Mo^{5+} spins. Therefore, it is very likely that the observation of the anomalous background in these compounds is ascribed to the incoherent interlayer transport due to the electron scattering by the Mo^{5+} magnetic moments in the intercalate layers. This interpretation agrees with a 2D band model treating the interlayer transport as a hopping mechanism,^{17,18,23,24} i.e., the carriers stay mostly in the graphite basal plane and occasionally transfer to the adjacent graphite layers crossing an intercalate layer by an interlayer hopping or to the neighboring graphite layers.

The observed peak at $\theta=90^\circ$ in higher-stage compounds is seemingly inconsistent with the anomalous background because a peak at $\theta=90^\circ$ arises from the coherent interlayer transport along the small closed orbits²⁹ or the self-crossing orbits³⁵ on the side of the corrugated cylindrical FS. On the assumption of a simple corrugation of the cylindrical FS, the interlayer transfer integral t_c can be estimated from the angle region $\Delta\theta_{\text{peak}}$, where

$$\Delta\theta_{\text{peak}} \approx \frac{2k_{\text{F}}t_c I_c}{E_{\text{F}}}. \quad (4)$$

If we assume a fully coherent case for the stage-5 MoCl_5 GIC, we obtain $t_c/E_{\text{F}} \sim 0.006$ from the experimental data $\Delta\theta_{\text{peak}}$ in Fig. 4(b) and $k_{\text{F}}=0.134 \text{ \AA}^{-1}$, respectively. The small value of t_c/E_{F} is consistent with the observation of the 2D FS's (Fig. 3). Assuming a parabolic energy band, the

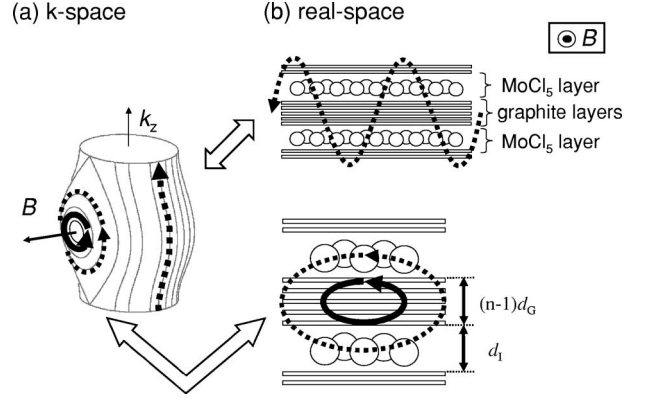


FIG. 7. Schematic picture of the coherent and incoherent transport for a stage-5 MoCl_5 GIC in (a) k space and (b) real space. Solid and dashed curves denote the trajectories corresponding to the coherent and incoherent transport, respectively.

Fermi energy is written as $E_{\text{F}} = \hbar^2 k_{\text{F}}^2 / 2\pi m_{\text{eff}}$, where A_{F} is the cross section of the Fermi surface. Using $m_{\text{eff}} = 0.12m_0$, we obtain $E_{\text{F}} \sim 577$ meV and then $t_c \sim 3.6$ meV. For a stage-4 MoCl_5 GIC, we also obtain almost the same value of $t_c/E_{\text{F}} \sim 0.006$ from the experimental data $\Delta\theta_{\text{peak}}$ and k_{F} .

In the range of a 2D band model with hopping conduction, the interlayer resistivity ρ_c can be expressed by^{17,18,23}

$$\rho_c \approx \frac{1}{I_c^{(n)}} [d_1 \rho_c(\text{GIG}) + (n-1)d_G \rho_c(\text{GG})], \quad (5)$$

where $I_c^{(n)}$ is the interlayer repeat distance of stage- n GIC, and $\rho_c(\text{GIG})$ and $\rho_c(\text{GG})$ are the resistivities associated with the carrier transfer across the graphite-intercalate-graphite sandwich layer and between nearest-neighbor graphite layers, respectively. $\rho_c(\text{GIG})$ makes a dominant contribution to ρ_c in lower-stage compounds while $\rho_c(\text{GG})$ term is important in higher-stage compounds. In stage- n ($n \geq 2$) GIC's, the i th graphite layer is assumed to be described by a 2D band with an effective mass m_i and then $\rho_c(\text{GG})$ is given by^{18,23}

$$\rho_c(\text{GG}) = \frac{1}{n-1} \sum_{i=1}^{n-1} \rho_{\text{GG}}(i, i+1), \quad (6)$$

where $\rho_{\text{GG}}(i, i+1)$ is the resistivity between the i th and $(i+1)$ th graphite layers. Because of the Coulomb screening effect, the transferred charge density of the bounding graphite layers next to the intercalate layer is larger than that of the interior graphite layers. Therefore, it is interpreted that the resistivity $\rho_{\text{GG}}(i, i+1)$ between the interior graphite layers dominantly contributes to $\rho_c(\text{GG})$ in higher-stage ($n \geq 4$) compounds. The stage dependence of $\rho_c(B)$ vs T has successfully been interpreted by this model.^{18,23,24}

The above model can also qualitatively explain both the anomalous background and a peak at $\theta=90^\circ$ observed in stages-4 and -5 MoCl_5 GIC's. We now concentrate on the magnetoresistance features in a stage-5 MoCl_5 GIC. Figures 7(a) and 7(b) depict the schematic picture of the coherent (solid arrows) and incoherent (dashed arrows) transport for a stage-5 MoCl_5 GIC in k space and in real space, respectively.

In this system, the MoCl₅ magnetic intercalates are accommodated regularly between five graphite layers. If the electrons are frequently scattered by these magnetic intercalates the interlayer transport should become incoherent. The upper part of Fig. 7(b) shows the excursion in real space corresponding to an open orbit trajectory on the side of the FS in a magnetic field at $\theta=90^\circ$ shown in Fig. 7(a). At low magnetic fields, the amplitude of the excursion is sufficiently large and the electrons are frequently scattered by the magnetic intercalates. As the field increases, the amplitude decreases monotonically and then becomes smaller than the graphite layers above the decoupling field. In this case, however, a finite incoherent hopping still remains along the interlayer direction. This incoherent motion, which can be expressed by the $\rho_c(\text{GIG})$ term in Eq. (5), may cause the anomalous background as discussed above. On the other hand, as long as the transport within the graphite layers is coherent, the Q2D FS's are well defined in the interior graphite layers. Indeed, the fact that combined frequencies are observed in the SdH oscillations indicates there are Fermi surfaces with different sizes in the same graphite layer and the electrons can coherently tunnel between the different FS's (magnetic breakdown effect). In this case, the closed orbital motion on the sides of the Q2D FS in k space can be realized for $\theta=90^\circ$, as shown in Fig. 7(a). Due to the highly anisotropic conductivity, the closed orbit also becomes highly elliptic along the k_z direction. In real space, if the diameter of the minor axes of the closed orbits becomes smaller than the thickness of graphite layers ($\approx 13.4 \text{ \AA}$ for a stage-5 MoCl₅ GIC), a peak at $\theta=90^\circ$ should be observable [lower part of Fig. 7(b)]. On the assumption of a simple corrugation of the cylindrical FS for $I_c=22.83 \text{ \AA}$ and $t_c\sim 3.6 \text{ meV}$, just for comparison, the diameter of the minor axis of the largest

closed orbit at $\theta=90^\circ$ is estimated as $\sim 250 \text{ \AA}$ at $B=10 \text{ T}$. It seems that the closed orbit only in the graphite layers gives a minor contribution to the peak and one may wonder whether a peak at $\theta=90^\circ$ can be observed. However, it is pointed out that making complete closed trajectories is not necessary for the observation of a peak at $\theta=90^\circ$.³⁶ Therefore, it is also very likely that the observation of a peak at $\theta=90^\circ$ is ascribed to the coherent interlayer transport only in the graphite layers, i.e., the $\rho_c(\text{GG})$ term in Eq. (5) is important in higher-stage compounds. This model also explains why a peak at $\theta=90^\circ$ is not observed in lower-stage compounds because the $\rho_c(\text{GIG})$ term rather than the $\rho_c(\text{GG})$ term in Eq. (5) makes a dominant contribution to ρ_c .

V. CONCLUSION

We have investigated the field-angle dependence of magnetoresistance for stages-2 to -5 MoCl₅ GIC's and revealed that all compounds have an anomalous background over the whole field region. The background can be attributed to incoherent interlayer transport due to the electron scattering by magnetic intercalates. On the other hand, a peak at $\theta=90^\circ$ becomes evident in higher-stage compounds, demonstrating coherent interlayer transport. The results are understood in terms of incoherent transport crossing the magnetic intercalate layers and coherent transport only in the graphite layers.

ACKNOWLEDGMENTS

The authors would like to express their sincere thank to Professor K. Sugihara and Dr. K. Takai for fruitful discussion. This work is supported by a Grant-in-Aid for Scientific Research from the Ministry of Education, Culture, Sports, Science and Technology of Japan (Grant No. 15073225).

*Electronic address: enomotti@mail2.accent.ne.jp

- ¹A. G. Lebed, JETP Lett. **43**, 174 (1986); G. M. Danner, W. Kang, and P. M. Chaikin, Phys. Rev. Lett. **72**, 3714 (1994); T. Osada, S. Kagoshima, and N. Miura, *ibid.* **77**, 5261 (1996).
- ²T. Ishiguro, K. Yamaji, and G. Saito, *Organic Superconductors*, 2nd ed. (Springer, Berlin, 1998).
- ³J. Singleton, Rep. Prog. Phys. **63**, 1111 (2000).
- ⁴R. H. McKenzie and P. Moses, Phys. Rev. Lett. **81**, 4492 (1998); P. Moses and R. H. McKenzie, Phys. Rev. B **60**, 7998 (1999).
- ⁵J. Wosnitzer, J. Hagel, J. S. Qualls, J. S. Brooks, E. Balthes, D. Schweitzer, J. A. Schlueter, U. Geiser, J. Mohtasham, R. W. Winter, and G. L. Gard, Phys. Rev. B **65**, 180506(R) (2002); J. Wosnitzer, J. Hagel, J. A. Schlueter, U. Geiser, J. Mohtasham, R. W. Winter, and G. L. Gard, Synth. Met. **137**, 1269 (2003).
- ⁶J. Singleton, P. A. Goddard, A. Ardavan, N. Harrison, S. J. Blundell, J. A. Schlueter, and A. M. Kini, Phys. Rev. Lett. **88**, 037001 (2002); J. Singleton, Synth. Met. **133**, 83 (2003).
- ⁷P. A. Goddard, S. J. Blundell, J. Singleton, R. D. McDonald, A. Ardavan, A. Narduzzo, J. A. Schlueter, A. M. Kini, and T. Sasaki, Phys. Rev. B **69**, 174509 (2004).
- ⁸H. Gutfreund and M. Weger, Phys. Rev. B **16**, 1753 (1977).
- ⁹S. P. Strong, D. G. Clarke, and P. W. Anderson, Phys. Rev. Lett.

73, 1007 (1994).

- ¹⁰G. M. Danner and P. M. Chaikin, Phys. Rev. Lett. **75**, 4690 (1995).
- ¹¹E. I. Chashechkina and P. M. Chaikin, Phys. Rev. Lett. **80**, 2181 (1998).
- ¹²T. Osada, H. Nose, and M. Kuraguchi, Physica B **294**, 402 (2001); M. Kuraguchi, E. Ohmichi, T. Osada, and Y. Shiraki, Synth. Met. **133**, 113 (2003).
- ¹³S. Uji, T. Terashima, S. Yasuzuka, J. Yamaura, H. M. Yamamoto, and R. Kato, Phys. Rev. B **68**, 064420 (2003).
- ¹⁴M. S. Dresselhaus and G. Dresselhaus, Adv. Phys. **30**, 139 (1981).
- ¹⁵T. Enoki, M. Suzuki, and M. Endo, *Graphite Intercalation Compounds and Applications* (Oxford University Press, New York, 2003).
- ¹⁶K. Sugihara, Phys. Rev. B **29**, 5872 (1984).
- ¹⁷K. Sugihara, Phys. Rev. B **37**, 4752 (1988).
- ¹⁸K. Sugihara, K. Matsubara, I. S. Suzuki, and M. Suzuki, J. Phys. Soc. Jpn. **67**, 4169 (1998).
- ¹⁹R. S. Markiewicz, Phys. Rev. B **37**, 6453 (1988).
- ²⁰R. Powers, A. K. Ibrahim, G. O. Zimmerman, and M. Tahar, Phys. Rev. B **38**, 680 (1988).

- ²¹M. Suzuki, A. Furukawa, H. Ikeda, and H. Nagano, *J. Phys. C* **16**, L1211 (1983).
- ²²M. Suzuki, L. J. Santodonato, I. S. Suzuki, B. E. White, and E. J. Cotts, *Phys. Rev. B* **43**, 5805 (1991).
- ²³M. Suzuki, C. Lee, I. S. Suzuki, K. Matsubara, and K. Sugihara, *Phys. Rev. B* **54**, 17128 (1996).
- ²⁴M. Suzuki, I. S. Suzuki, K. Matsubara, and K. Sugihara, *Phys. Rev. B* **61**, 5013 (2000); K. Matsubara, K. Sugihara, I. S. Suzuki, and M. Suzuki, *J. Phys.: Condens. Matter* **11**, 3149 (1999).
- ²⁵Y. Yoshida and S. Tanuma, *J. Phys. Soc. Jpn.* **54**, 701 (1985); **54**, 707 (1985).
- ²⁶W. R. Datars, J. D. Palidwar, T. R. Chien, P. K. Ummat, H. Aoki, and S. Uji, *Phys. Rev. B* **53**, 1579 (1996).
- ²⁷D. Shoenberg, *Magnetic Oscillations in Metals* (Cambridge University Press, Cambridge, U.K., 1984).
- ²⁸V. A. Kulbachinskii, S. G. Ionov, S. A. Lapin, and A. deVisser, *Phys. Rev. B* **51**, 10313 (1995).
- ²⁹N. Hanasaki, S. Kagoshima, T. Hasegawa, T. Osada, and N. Miura, *Phys. Rev. B* **57**, 1336 (1998); **60**, 11210 (1998).
- ³⁰K. Kajita, Y. Nishio, T. Takahashi, W. Sasaki, R. Kato, H. Kobayashi, A. Kobayashi, and Y. Iye, *Solid State Commun.* **70**, 1189 (1989).
- ³¹K. Yamaji, *J. Phys. Soc. Jpn.* **58**, 1520 (1989).
- ³²H. Sato, O. E. Andersson, T. Enoki, I. S. Suzuki, and M. Suzuki, *J. Phys. Soc. Jpn.* **69**, 1136 (2000).
- ³³P. A. Dube, M. Barati, P. K. Ummat, G. Luke, and W. R. Datars, *J. Phys.: Condens. Matter* **15**, 203 (2003).
- ³⁴Y. Iye, M. Baxendale, and V. Z. Mordkovich, *J. Phys. Soc. Jpn.* **63**, 1643 (1994); Y. Iye, *Mater. Sci. Eng., B* **31**, 141 (1995).
- ³⁵V. G. Peschansky and M. V. Kartsovnik, *Phys. Rev. B* **60**, 11207 (1999).
- ³⁶M. V. Kartsovnik, *Chem. Rev. (Washington, D.C.)* **104**, 5737 (2004).